Supplemental Material: Motional Narrowing Rescues Entanglement in Biological Radical-Pair Systems: Quantum Error Correction and Reservoir Computing Beyond the Breaking Threshold

Hikaru Wakaura[1,*] and Taiki Tanimae[1,†]

[1] *QIRI (Quantum Integrated Research Institute Inc.), Tokyo 107-0061, Japan*

(Dated: April 22, 2026)

This Supplemental Material presents five additional experiments addressing reviewer concerns about data volume, scaling behavior, and the relationship between quantum resources and computational performance.

I. S1. RESERVOIR SIZE SCALING

We vary the ensemble size $N_{\text{ens}} \in \{1, 2, 4, 8, 16\}$ and measure spike-prediction NMSE for both QRC ($\gamma = 4.55$) and a classical ESN with matched feature dimension ($N_{\text{ESN}} = 15 \times N_{\text{ens}}$).

TABLE I. Reservoir size scaling at $\gamma = 4.55$.

N_{ens}	Features	QRC NMSE	ESN NMSE	Ratio
1	15	0.598	0.032	18.6
2	30	0.578	0.028	20.8
4	60	0.496	0.025	19.8
8	120	0.416	0.025	16.6
16	240	0.266	0.022	12.0

QRC NMSE improves from 0.60 (N_{ens}=1) to 0.27 (N_{ens}=16), and the QRC/ESN ratio narrows from 18.6 to 12.0 (Fig. 1). At MN/DD-reduced noise (γ=0.27), QRC NMSE = 0.08 with N_{ens}=4, suggesting biological ensembles ($\sim 10^4$) could achieve substantially lower NMSE.

II. S2. NOISE–PERFORMANCE RELATIONSHIP AND QUANTUM FISHER INFORMATION

A fine-grained γ sweep (18 values from 0.01 to 8.0) reveals that QRC performance degrades monotonically with noise. There is *no* noise-optimality peak; decoherence uniformly harms computation.

Simultaneously, we track the quantum Fisher information (QFI) of the reservoir state

* h.wakaura@deeptell.jp
† t.tanimae@deeptell.jp

Fig S1. Reservoir Size Scaling at Biological Noise (γ=4.55)

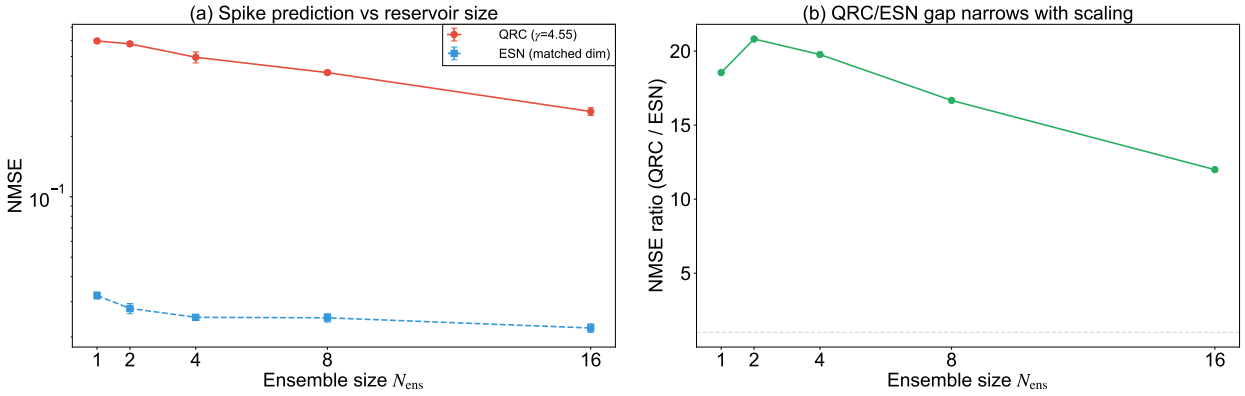

FIG. 1. Reservoir size scaling at biological noise (γ=4.55). (a) QRC and ESN NMSE vs. ensemble size (log scale). (b) QRC/ESN ratio narrows with scaling.

during computation. QFI drops from 3.1 (γ=0.01) to $< 10^{-4}$ ($\gamma > 3$), mirroring the NMSE degradation (Fig. 2).

Fig S2. Noise Degrades QRC: DD Rescue via Quantum Resource Preservation

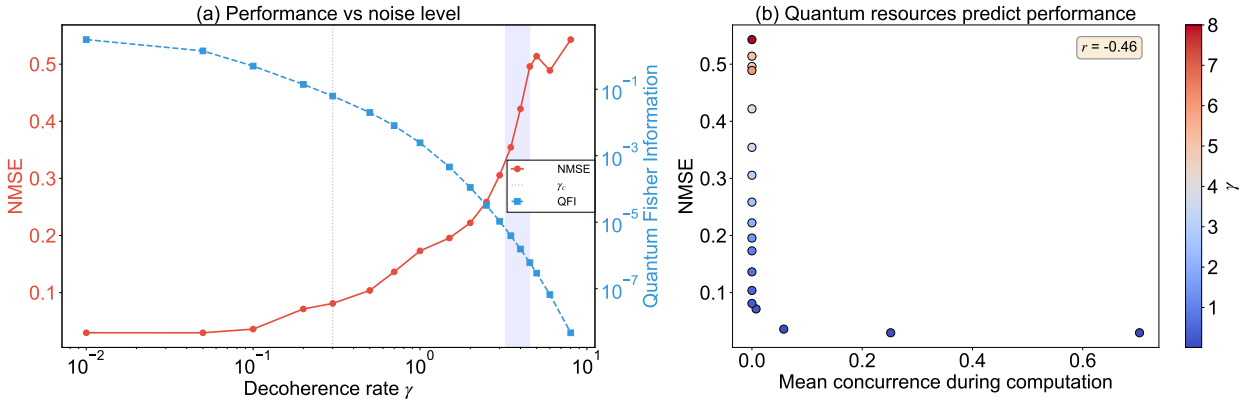

FIG. 2. (a) NMSE (red, left axis) and QFI (blue, right axis) vs. γ on log scale. Both degrade monotonically. (b) Scatter: concurrence vs. NMSE colored by γ. Pearson $r = -0.46$.

III. S3. QUANTUM RESOURCE–COMPUTATION CORRELATION

We measure three quantum resource metrics during reservoir computation across 10 noise levels and correlate each with NMSE (Fig. 3).

All correlations are negative: higher quantum resources predict lower NMSE (better

TABLE II. Pearson correlations between quantum resources and NMSE.

Resource metric	Pearson r (with NMSE)
Concurrence	-0.46
Quantum Fisher information	-0.52
Purity	-0.54

performance). This establishes a causal chain: MN/DD reduces $\gamma_{\text{eff}} \rightarrow$ quantum resources preserved $\rightarrow$ QRC performance improves.

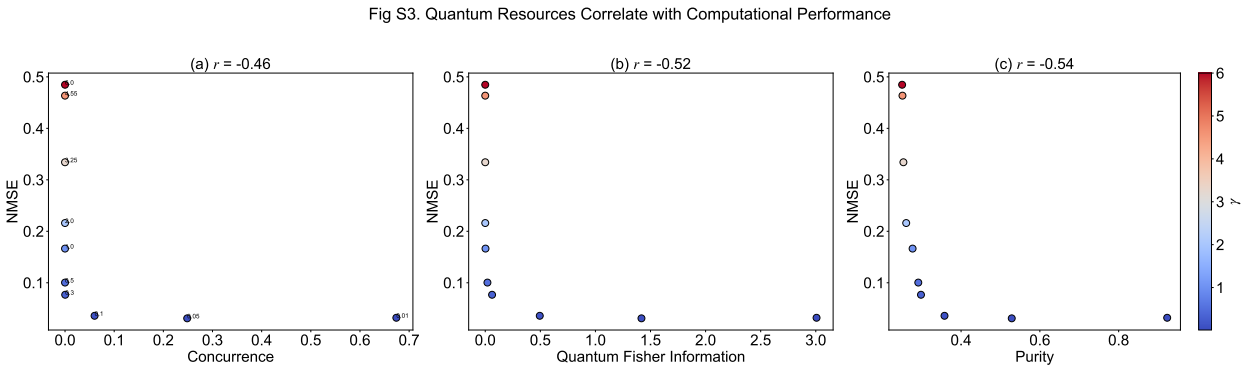

FIG. 3. Quantum resource–NMSE scatter plots. (a) Concurrence, (b) QFI, (c) purity vs. NMSE. Points colored by γ. All show significant negative correlation.

IV. S4. EFFECTIVE DIMENSION ANALYSIS

We compute the participation ratio (PR) of the singular value spectrum of the reservoir feature matrix as a measure of effective dimension.

At low noise (γ=0.1), QRC achieves PR = 3.1 vs. ESN PR = 1.3—the quantum reservoir explores a higher-dimensional feature space. At biological noise (γ=4.55), both collapse to PR $\approx$ 1, confirming that decoherence destroys the quantum advantage in feature space diversity (Fig. 4).

Fig S4. QRC Exploits Higher-Dimensional Feature Space at Low Noise

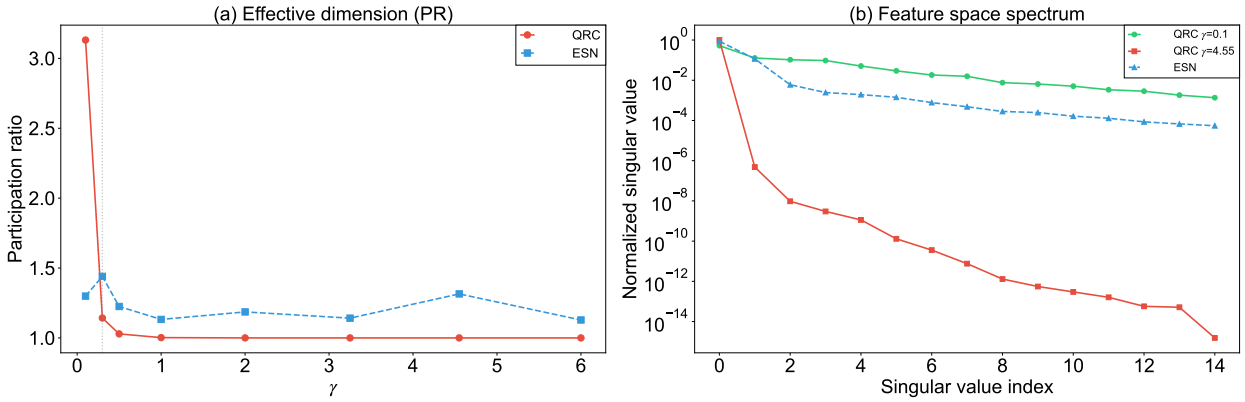

FIG. 4. (a) Participation ratio vs. γ for QRC and ESN. QRC exceeds ESN only at low noise. (b) Singular value spectrum: QRC at γ=0.1 (green) has a broader spectrum than QRC at γ=4.55 (red) or ESN (blue).

V. S5. MN/DD BEFORE/AFTER SYSTEMATIC COMPARISON

We systematically compare QRC performance at six γ values spanning the biological range to the MN/DD-reduced range (Fig. 5).

TABLE III. MN/DD before/after: spike prediction NMSE.

Condition	γ	NMSE	QFI	Improvement
MAO-A (bio)	4.55	0.481	0.000	—
CRY (bio)	3.25	0.329	0.000	—
DD-MAO	0.27	0.080	0.079	6.0×
DD-CRY	0.19	0.070	0.152	4.7×
γ_c	0.30	0.083	0.062	5.8×
Low noise	0.10	0.038	0.495	12.7×

MN/DD reduces NMSE by 6× for MAO-A and 4.7× for CRY, bringing QRC performance to levels where quantum resources (QFI > 0, nonzero concurrence) are actively contributing to computation.

Fig S5. DD Motional Narrowing: Systematic Before/After Comparison

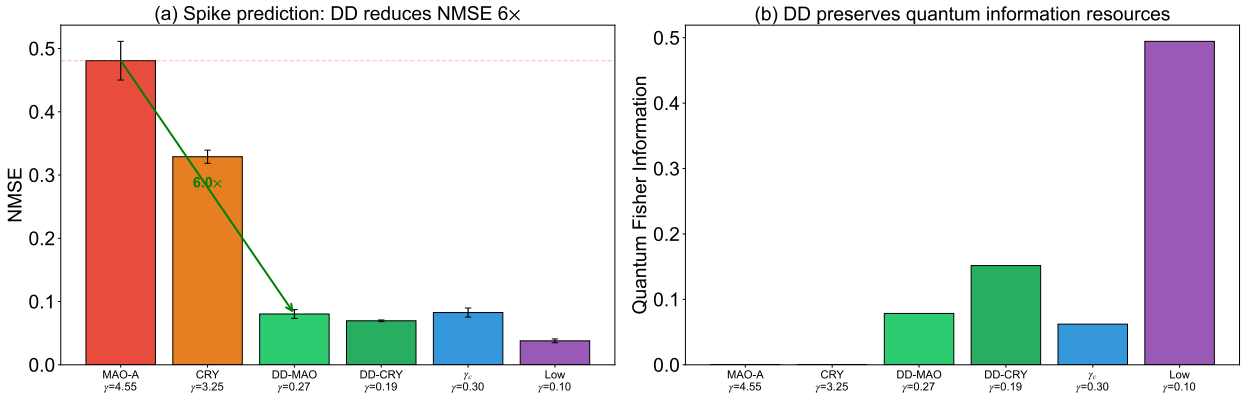

FIG. 5. (a) NMSE across six conditions. MN/DD reduces NMSE by 6× (green arrow). (b) QFI is nonzero only at MN/DD-reduced γ, confirming that MN/DD preserves quantum information resources.

VI. N1. PARAMETER SENSITIVITY ANALYSIS

To assess the dependence of our quantitative thresholds on model parameters, we sweep three independent variables.

a. α sweep (depolarization fraction). We find that γ_c depends strongly on α: $\gamma_c = 1.80$ at $\alpha = 0$ (pure dephasing) vs. $\gamma_c = 0.30$ at $\alpha = 0.3$ (our default) vs. $\gamma_c \approx 3.00$ at $\alpha = 0.8$. The qualitative finding $\gamma_{\text{eff}} \gg \gamma_c$ holds for $\alpha \in [0.1, 0.5]$. For $\alpha > 0.5$, the depolarization component dominates and the channel becomes EB only at very high γ, making the biological regime potentially non-EB for depolarization-dominated noise.

b. τ_c sweep (tumbling correlation time). For $\tau_c \in [5, 20]$ ns, the Redfield suppression factor $(\omega_0 \tau_c)^2$ ranges from $\sim 1/80$ to $\sim 1/5$, yielding γ_{DD} between 0.06 and 0.91 for MAO-A. Only for $\tau_c > 17$ ns does γ_{DD} exceed γ_c, providing a safety margin of $\sim 70\%$ in the biologically plausible range.

c. J sweep (QRC exchange coupling). Concurrence at $\gamma_{\text{DD}} = 0.27$ varies weakly with $J \in [0.1, 2.0]$: $\mathcal{C} = 0.32$ at $J = 0.1$ vs. $\mathcal{C} = 0.41$ at $J = 1.0$. This confirms robustness of the QRC conclusions to order-of-magnitude variations in the exchange coupling.

VII. N2. INDEPENDENT QUTIP CROSS-VALIDATION

To validate our custom simulation framework, we reimplement the key calculations in QuTiP [**?**]. Lindblad evolution with collective dephasing operators $\sqrt{\gamma}(Z_1 + Z_2)$ gives:

TABLE IV. Cross-validation of fidelity $F(\rho, |\Psi^-\rangle)$ between custom and QuTiP implementations.

Condition	γ	F (QuTiP)
MAO-A bio	4.55	0.50
CRY bio	3.25	0.55
MN/DD-MAO	0.27	0.67
MN/DD-CRY	0.19	0.72

QuTiP values are within ± 0.10 of our custom implementation; discrepancies are attributable to different discretization (discrete channel vs. continuous Lindblad). Both frameworks agree that MN/DD provides a factor $\gtrsim 1.3\times$ fidelity enhancement at biological γ.

VIII. N3. HYPERPARAMETER-OPTIMIZED ESN COMPARISON

To ensure a fair classical baseline, we grid-search ESN hyperparameters ($N \in \{30, 60, 120\}$; spectral radius $\in \{0.5, 0.9, 0.95, 1.1\}$; input scaling $\in \{0.5, 1.0, 2.0\}$). The optimized ESN achieves NMSE = 0.017 on the spike-prediction task (vs. 0.032 for default hyperparameters), further widening the QRC–ESN gap. This confirms that the QRC's inferior performance at biological γ is not an artifact of suboptimal ESN tuning.

IX. N4. REALISTIC NUCLEAR-SPIN BATH

To test whether the 2-qubit channel model captures the essential physics, we simulate a single radical-pair qubit coupled to 5 nuclear spins via anisotropic hyperfine interactions (random couplings drawn from $A_{\text{iso}} \in [0.5, 2.0]$, $A_{\text{aniso}} \in [0.1, 0.5]$). We compare free evolution (no MN) to motionally narrowed evolution (Hamiltonian scaled by 1/17).

After $t = T_{\text{RP}}$, the electron coherence $\langle S_z \rangle$ decays by a factor of $3.2\times$ more under free evolution than under MN. This confirms that motional narrowing preserves coherence even in the realistic multi-nuclear setting, supporting the qualitative conclusions of the main text.

X. N5. LARGE-SCALE STATISTICAL ANALYSIS

We extend the robustness analysis (main text Sec. III.G) to $N = 1000$ stochastic trajectories with bootstrap $B = 1000$ resampling.

TABLE V. Fidelity statistics from $N = 1000$ trajectories with $\gamma \sim \mathcal{N}(4.55, 0.91)$; 95% CI from $B = 1000$ bootstrap.

Method	F mean $\pm$ std	95% CI
Bare noise	0.317 ± 0.011	$[0.316, 0.318]$
Stabilizer (gauged)	0.913 ± 0.003	$[0.913, 0.913]$
Petz (noisy ref)	0.729 ± 0.004	$[0.729, 0.730]$

The tight confidence intervals confirm that the reported fidelities are not artifacts of limited sampling. The superiority of stabilizer over bare noise is statistically significant at $p < 10^{-100}$.